

## Decharging of Complex Plasmas: First Kinetic Observations

A. V. Ivlev,<sup>1</sup> M. Kretschmer,<sup>1</sup> M. Zuzic,<sup>1</sup> G. E. Morfill,<sup>1</sup> H. Rothermel,<sup>1</sup> H. M. Thomas,<sup>1</sup> V. E. Fortov,<sup>2</sup> V. I. Molotkov,<sup>2</sup>  
A. P. Nefedov,<sup>2</sup> A. M. Lipaev,<sup>2</sup> O. F. Petrov,<sup>2</sup> Yu. M. Baturin,<sup>3</sup> A. I. Ivanov,<sup>4</sup> and J. Goree<sup>5</sup>

<sup>1</sup>Centre for Interdisciplinary Plasma Science, Max-Planck-Institut für Extraterrestrische Physik, D-85740 Garching, Germany

<sup>2</sup>Institute for High Energy Densities, RAS, 125412 Moscow, Russia

<sup>3</sup>Yuri Gagarin Cosmonauts Training Center, 141160 Star City, Moscow Region, Russia

<sup>4</sup>RSC "Energia," 141070 Korolev, Russia

<sup>5</sup>Department of Physics and Astronomy, The University of Iowa, Iowa City, Iowa 52242

(Received 3 June 2002; published 4 February 2003)

The first experiment on the decharging of a complex plasma in microgravity conditions was conducted. After switching off the rf power, in the afterglow plasma, ions and electrons rapidly recombine and leave a cloud of charged microparticles. Because of microgravity, the particles remain suspended in the experimental chamber for a sufficiently long time, allowing precise measurements of the rest particle charge. A simple theoretical model for the decharging is proposed which agrees quite well with the experiment results and predicts the rest charge at lower gas pressures.

DOI: 10.1103/PhysRevLett.90.055003

PACS numbers: 52.27.Lw, 82.33.Xj

Complex (dusty) plasmas consist of an overall charge neutral assembly of ions, electrons, and charged microparticles. The latter are visible individually and allow experiments in plasma science at the kinetic level with high temporal and spatial resolution (in terms of the appropriate plasma frequency and particle separation) [1–9]. This tremendous advance also has a drawback—gravity (which normally plays no role in usual plasmas) is an important force in these systems. Experiments under microgravity can overcome this problem.

The PlasmaKristall experiment ("PKE-Nefedov") is the first natural science laboratory in operation on the International Space Station [10,11]. Its mission is to study basic phenomena occurring in complex plasmas under microgravity conditions, such as structures and transitions in plasma crystals [10], waves and shocks [12], formation and interaction of complex plasma boundaries [13], etc. Very important is the study of the particle charging processes in a wide range of experimental parameters [9,14,15]. In this Letter we report an experiment where the decay, or "decharging" of a complex plasma in the afterglow, after switching off the discharge power was investigated.

The PKE-Nefedov experimental setup [11] is a development from an earlier TEXUS-36 microgravity experiment [6]. Microparticles of two sizes can be introduced into a rf chamber (filled with argon gas); for the experiment discussed here, we used melamine-formaldehyde particles with a diameter of 6.8  $\mu\text{m}$ . The particles were illuminated by a vertical laser sheet of  $\approx 140 \mu\text{m}$  thickness and imaged from the side with a video camera at a rate of 25 frame/s. After injection the particles are charged rapidly and form a cloud with an ellipsoidal void in the center of the chamber, as shown in Fig. 1(a). The shape of the cloud is close to that observed earlier in the TEXUS-36 experiments [6]. In order to study the particle charges a sinusoidal voltage produced by a func-

tion generator (FG) with amplitude  $\pm 13 \text{ V}$  and frequency 0.47 Hz was applied (out of phase) to the upper and lower electrodes. This caused vertical oscillations of the cloud due to the electrode sheath modulation. The FG voltage was applied only to the outer part of the electrodes (outer rings, see Fig. 1); the particle dispensers in the center were grounded. Also, the lower ring was biased negatively (about 2–3 V) with respect to the upper ring. For this experiment, the neutral gas pressure was  $p = 73 \text{ Pa}$ ; the rf peak-to-peak voltage was  $\approx 90 \text{ V}$ . The plasma number density in the bulk was estimated using a 2D fluid code [16] yielding  $n_0 \sim 3 \times 10^9\text{--}10^{10} \text{ cm}^{-3}$ , the particle density in the cloud is of the order of  $N \sim 3 \times 10^4\text{--}10^5 \text{ cm}^{-3}$ , and the particle charge  $Z_0 \sim 10^4 e$  is evaluated from the orbital motion limited (OML) approach [17].

After the discharge was switched off, the afterglow plasma disappeared during a few milliseconds and the cloud slowly drifted upward [Figs. 1(b) and 1(c)]. One of the causes for the drift is believed to be the thermophoretic force—the lower electrode was  $\sim 1^\circ$  hotter than the upper one (heat release from the electronics mounted under the chamber). We studied the dynamics of the cloud ("layer" below the void) in detail. The vertical motion of different parts of the layer is strongly dependent on the radial (horizontal) position: Figure 2 shows the vertical position (center of masses) of the layer versus time in the center and at the "periphery" (as marked in Fig. 1). The first obvious feature is that the drift velocity increases with radial distance from the chamber axis; the second one is that the particles oscillate at the FG frequency with amplitudes which are also higher at the periphery. Since the vertical ac and dc electric fields also increase with radial distance, both observed features have a clear electric nature, i.e., the particles retained a certain negative charge after the plasma was off. Hence, the total force on the particles is a combination of thermophoretic and

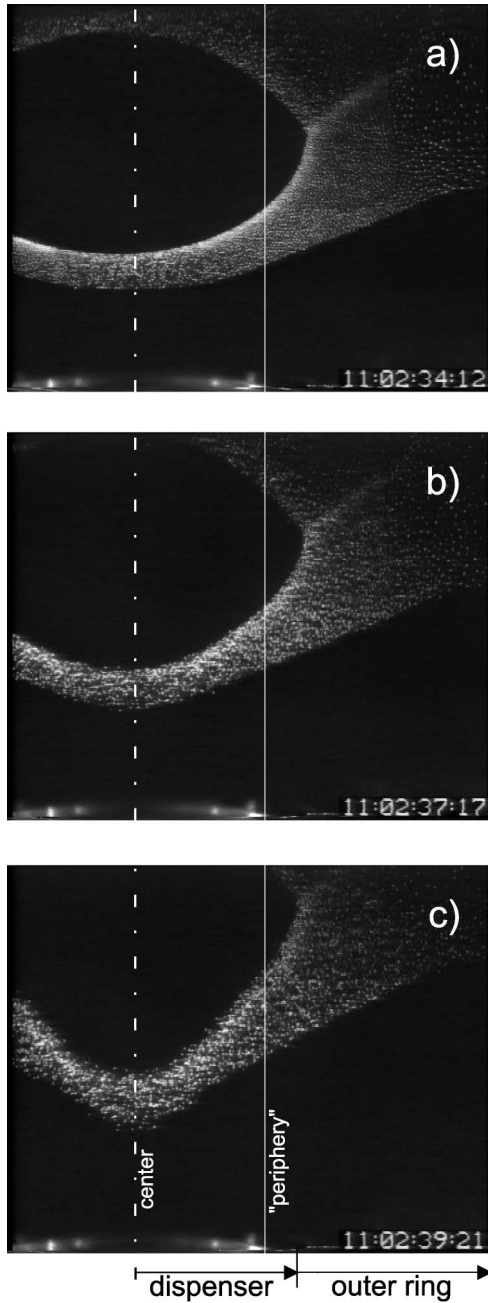


FIG. 1. Cross section side view of the complex plasma particle cloud. The cloud is shown before (a) and after (b),(c) the rf discharge was switched off. The density wave fronts seen in (a) are result of the electrode sheath modulation. Snapshots (b) and (c) are made  $\approx 2$  and  $\approx 4$  sec after switching off the rf power and show the vertical motion of the lower part of the cloud. The surface of the lower electrode coincides with the lower edge of the figures (the upper electrode is beyond the upper edge). The inner part of the electrode with the central axis (cylindrical dispenser) and the outer ring are indicated.

electrostatic forces balanced by the neutral friction (“Epstein” drag, terminal drift velocity  $\approx 1\text{--}2$  mm/s is reached in  $\sim 3$  ms). We can determine the rest charge on the microparticles using the measured amplitude of oscillations,  $A$ , and the relation derived from the equation of

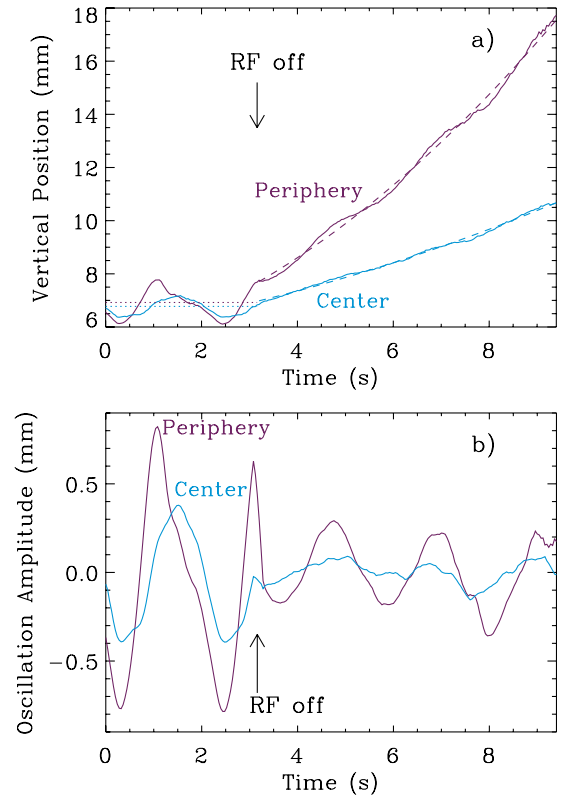


FIG. 2 (color online). (a) Vertical position (center of masses) of the lower part of the particle cloud as indicated in Fig. 1. The two curves show the vertical motion in the center and at the periphery (as marked in Fig. 1) of the experimental chamber. The motion is a combination of the quasi-steady vertical drift (dashed line) and the oscillations with the FG frequency. (b) Oscillatory part of the motion.

motion,  $A = eZ_{\text{rest}}E_{\text{FG}}/(2\gamma\omega M)$ . Typical amplitude at the periphery was  $A \approx 0.2\text{--}0.3$  mm; the excitation FG electric field  $E_{\text{FG}} \approx 8\text{--}10$  V/cm had frequency  $\omega = 2\pi f_{\text{FG}} = 2.95$  s $^{-1}$ . Particles of mass  $M \approx 2.5 \times 10^{-10}$  g have a neutral gas drag damping coefficient  $2\gamma \approx 140$  s $^{-1}$ . Then we obtain that each particle carried  $Z_{\text{rest}} \approx 130\text{--}150$  electron charges. This “rest charge” (which particles kept after the discharge was switched off) is about 2 orders of magnitude less than the initial (plasma) value, but is still a quite significant charge. In order to explain this effect, we propose a simple model of the complex plasma discharging. We study the plasma decay after the discharge power is turned off and include the self-consistent variation of the particle charge. It is assumed that the density of particles is sufficiently low and they do not change the initial plasma charge composition.

The kinetics of the plasma decay is determined by the plasma recombination (loss) and the electron temperature relaxation. Loss of the plasma is due to a combination of diffusion onto the walls of the discharge chamber [18] and surface recombination (absorption) on the particles [17,19]. At the initial stage of the decay, the plasma is quasineutral,  $n_i \approx n_e$ . The equation for the dimensionless plasma density  $\tilde{n} = n_{i,e}/n_0$  is [18]

$$d\tilde{n}/dt = -\tilde{n}/\tau_L, \quad (1)$$

where  $\tau_L$  is the time scale of the plasma loss,  $\tau_L^{-1} = \tau_D^{-1} + \tau_A^{-1}$ . The diffusion time scale  $\tau_D$  is determined by the ambipolar diffusion flux onto the walls, which is inversely proportional to the squared characteristic diffusion length  $\Lambda^2$  [for cylindrical geometry,  $\Lambda^{-2} \approx (\pi/H)^2 + (2.4/R)^2$ , where  $H$  and  $R$  are the height and the radius of the cylinder]. The absorption time scale  $\tau_A$  is determined by the flux onto the particles, which is proportional to the total particle surface,  $\pi a^2 N$ . Introducing the thermal velocity of ions  $v_{T_i} = \sqrt{T_i/m_i}$  and the mean free path of ion-neutral collisions  $l_{in}$ , we get the following explicit expressions for the loss time scales [17,18]:

$$\begin{aligned} \frac{1}{\tau_D} &\approx \frac{2\sqrt{2}l_{in}v_{T_i}}{3\sqrt{\pi}\Lambda^2} (1 + \tilde{T}_e) \equiv \frac{1}{2} (1 + \tilde{T}_e) \frac{1}{\tau_D^\infty}, \\ \frac{1}{\tau_A} &\approx 2\sqrt{2}\pi a^2 N v_{T_i} (1 + z\tilde{T}_e) \equiv \left( \frac{1+z\tilde{T}_e}{1+z} \right) \frac{1}{\tau_A^\infty}. \end{aligned} \quad (2)$$

Here  $\tilde{T}_e = T_e/T_n$  is the ratio of the electron to neutral temperatures; the ion and neutral temperatures are assumed to be equal,  $T_i = T_n \equiv T$ . The parameter  $z \sim 3$  (which has a weak dependence on  $\tilde{T}_e$ ) is defined below. The initial electron temperature is much higher than  $T$  (typically,  $\tilde{T}_{e0} \sim 10^2$ ), but after switching off the power it starts decreasing due to energy exchange in collisions with neutrals and tends asymptotically to  $T$ . Therefore, the diffusion time scale increases with time, from the initial value  $\tau_D^0 \approx (2/\tilde{T}_{e0})\tau_D^\infty$  to the limit  $\tau_D^\infty$ . The absorption time scale has a similar dependence on the temperature and grows from  $\tau_A^0 \approx [(1+z^{-1})/\tilde{T}_{e0}]\tau_A^\infty$  up to  $\tau_A^\infty$ . Thus, the overall plasma loss time scale increases by a factor  $\sim \tilde{T}_{e0}$ , from  $\tau_L^0$  up to  $\tau_L^\infty$ . The equation of the electron temperature relaxation is [18]

$$d\tilde{T}_e/dt = -(\tilde{T}_e - 1)/\tau_T. \quad (3)$$

The time scale of the temperature relaxation is

$$\frac{1}{\tau_T} = 2\sqrt{\frac{m_e}{m_i}} \frac{v_{T_i}}{l_{en}} \sqrt{\tilde{T}_e} \equiv \frac{\sqrt{\tilde{T}_e}}{\tau_T^\infty}. \quad (4)$$

Hence,  $\tau_T$  also grows with time, from  $\tau_T^0 = \tau_T^\infty/\sqrt{\tilde{T}_{e0}}$  to  $\tau_T^\infty$ .

The particle charge number  $Z$  is a function of the electron and ion densities and the electron temperature. The kinetic equation for  $Z$  in the orbital motion limit (OML) is [19]

$$\begin{aligned} dZ/dt &= J_e - J_i \\ &\equiv 2\sqrt{2}\pi a^2 [n_e v_{T_e} e^{-z} - n_i v_{T_i} (1 + \tilde{T}_e z)], \end{aligned} \quad (5)$$

where  $J_{e,i}$  are the electron and ion fluxes on the particles and  $z = e^2 Z/aT_e$  is the dimensionless surface potential of the particle [this parameter is used to determine  $\tau_A$  in Eq. (2)]. If the time scale of the charge fluctuations is sufficiently short (less than  $\tau_L$  and  $\tau_T$ ), then the charge is

close to equilibrium,  $z \approx z_{\text{eq}}$ . In this case, ion and electron fluxes balance each other (which determines the value of  $\tau_A$ ), and  $z_{\text{eq}}$  is given by

$$(n_e/n_i)\sqrt{\tilde{T}_e} e^{-z_{\text{eq}}} = \sqrt{m_e/m_i} (1 + \tilde{T}_e z_{\text{eq}}). \quad (6)$$

Note that  $z_{\text{eq}}$  is a function of three parameters—the electron-ion density ratio, temperature ratio, and mass ratio. The dependence on  $T_e$  (as well as on  $m_e/m_i$ ) is very weak. For example, for quasineutral Ar plasma  $z_{\text{eq}}(\tilde{T}_e)$  increases from  $\approx 2.4$  up to  $\approx 4.0$  when  $\tilde{T}_e$  drops down from  $10^2$  to unity. The equation for the charge fluctuations around equilibrium is derived from Eq. (5), yielding  $dZ/dt \approx -(Z - Z_{\text{eq}})/\tau_Z$ , with the fluctuation time scale  $\tau_Z$ , which increases monotonically as the plasma density decays,

$$\frac{1}{\tau_Z} \approx \frac{v_{T_i} a}{\sqrt{2}\pi\lambda_{i0}^2} (1 + z_{\text{eq}}) \tilde{n} \equiv \frac{\tilde{n}}{\tau_Z^0}, \quad (7)$$

( $\lambda_{i0} = \sqrt{T/4\pi n_0 e^2}$  the initial ion Debye length). Thus, if  $\tau_Z \lesssim \min\{\tau_T, \tau_L\}$ , then the charge fluctuates around the equilibrium value [Eq. (6)], with the time scale  $\tau_Z$ . In the opposite case, the general kinetic equation for the charge, Eq. (5), should be used.

The differential Eqs. (1), (3), and (5) along with the plasma quasineutrality condition and Eqs. (2), (4), and (7) for the time scales is a complete set of equations describing the decay of a complex plasma in general. For our experiment, we assume an initial temperature ratio  $\tilde{T}_{e0} = 100$  and a diffusion length  $\Lambda \sim 0.5\text{--}1$  cm. Then the hierarchy of the initial time scales is  $\tau_Z^0 \sim 1$   $\mu\text{s}$  and  $\tau_T^0 \sim \tau_L^0 \sim 30\text{--}60$   $\mu\text{s}$ . Hence, the initial charge  $Z_0$  is in equilibrium. After switching off the discharge, the electron temperature drops down to room temperature (or,  $\tilde{T}_e \rightarrow 1$ ) in a time  $\sim \tau_T^\infty = \sqrt{\tilde{T}_{e0}}\tau_T^0 \sim 10\tau_T^0$ . At the same time, the plasma density remains almost unchanged: The plasma recombination slows down due to the temperature decrease and the loss time scale increases up to  $\tau_L^\infty \sim \tilde{T}_{e0}\tau_L^0 \sim 100\tau_L^0$ . The charging time scale does not depend on  $\tilde{T}_e$  [see Eq. (7)], so that  $\tau_Z = \tau_Z^0$  and the charge is still determined by the equilibrium value  $z_{\text{eq}}$  from Eq. (6). Since  $Z_{\text{eq}} \propto \tilde{T}_e z_{\text{eq}}(\tilde{T}_e)$ , we get that at  $t \sim \tau_T^\infty$  the particle charge decreases asymptotically to the value  $Z_{\text{eq}} = \tilde{T}_{e0}^{-1} [z_{\text{eq}}(1)/z_{\text{eq}}(\tilde{T}_{e0})] Z_0 \approx 1.6 \times 10^{-2} Z_0$ . At  $t \geq \tau_L^\infty$  the density starts decreasing as  $\tilde{n} \propto e^{-t/\tau_L^\infty}$  in accordance with Eq. (1) and  $\tau_Z$  grows exponentially [see Eq. (7)]. However, as long as the plasma is quasineutral, the charge (which is a function of  $n_i/n_e$ ) cannot change at this stage. If the particle volume charge  $ZN$  is neglected, the plasma quasineutrality is violated when the Debye length becomes comparable with the chamber size,  $\lambda_i(\tilde{n}_*) \sim \Lambda$ , i.e., when the density drops down to  $\tilde{n}_* \sim \lambda_{i0}^2/\Lambda^2$ . This occurs at  $t_* \sim \tau_L^\infty \ln \tilde{n}_*^{-1}$ . At  $t \geq t_*$  electrons and ions start diffusing independently, the ratio  $n_i/n_e$  grows, and therefore the relative contribution of the ion flux in Eq. (5)

increases. Using the scaling,  $J_i \sim a^2 n_i v_{Ti} (1 + \tilde{T}_{e0} z) \sim z^{-1} (Z/\tau_Z)$ , we estimate the charge variation at this stage as follows:  $|dZ/dt| < J_i \sim z_{\text{eq}}^{-1} [Z_{\text{eq}}/\tau_Z(t_*)] e^{-(t-t_*)/\tau_L^0}$ . From this inequality we evaluate the upper limit of the relative change of the charge at  $t \geq t_*$  as  $|Z - Z_{\text{eq}}|/Z_{\text{eq}} \leq \tau_L^0/\tau_Z(t_*)$ . Using Eqs. (2) and (7) we get that this change is less than  $a/l_{in}$  which is  $\sim 10^{-2}$  for micron size particles and millibarn pressures. Therefore, the charge variation at the last stage is negligible because  $\tau_Z(t_*)$  exceeds significantly the time scale of the density decay — the charge cannot follow the density variations in the ambient plasma and becomes “frozen.” We finally conclude that the rest particle charge  $Z_{\text{rest}}$  should be about  $1.6 \times 10^{-2} Z_0 \approx 160e$ , which is in very good agreement with the measured value.

Let us consider how the time scales depend on the rf plasma parameters, assuming that the characteristics of the particle cloud (particle number density and particle size) are fixed. Since  $\tilde{T}_{e0}$  is typically about  $10^2$ , the major parameter that can be varied significantly is the gas pressure  $p$ . Both the charging and the temperature relaxation processes accelerate with pressure  $-\tau_Z, \tau_T \propto p^{-1}$ , whereas the plasma loss has the opposite tendency  $-\tau_D \propto p$ , and  $\tau_A$  does not depend on  $p$ . The initial charging time for micron size particles is usually much shorter than the time of the temperature relaxation: Using Eqs. (4) and (7) we get  $\tau_Z^0/\tau_T^0 \sim 10^{-1}-10^{-2}$ . Thus, initially charging is the fastest process. Then we compare the temperature relaxation and the plasma loss processes: Using Eqs. (2) and (4), we get  $\tau_T \sim \tau_L$  at  $p_{\text{cr}} \sim 30-100$  Pa. Hence, in the limit of very low pressures,  $p \ll p_{\text{cr}}$ , the temperature relaxation can be the slowest process,  $\tau_L^0 \ll \tau_T^0$ . In this case, after switching off the discharge the plasma density decreases as  $e^{-t/\tau_L^0}$  up to  $t \leq \tau_T^0$  (the charging time correspondingly increases), whereas the temperature (and thus the charge) remains constant. The charge can start changing only at  $t \geq \tau_T^0$ . However, the charge can be already frozen at this moment, if  $\tau_L/\tau_Z \leq 1$ . This condition can be rewritten as  $(\tau_L^0/\tau_Z^0) e^{-\tau_T^0/\tau_L^0} \leq 1$ . Since  $\tau_L^0/\tau_Z^0 \propto p^2$  and  $\tau_T^0/\tau_L^0 \propto p^{-2}$  (at low pressures  $\tau_L \approx \tau_D \propto p$ ), the condition can be easily satisfied for sufficiently small  $p$ . Thus, a possible scenario for very low pressures is that the rest particle charge might be frozen at or near the initial “plasma level,”  $Z_{\text{rest}} \approx Z_0$ .

In our model, we neglected the influence of the volume particle charge on the process, assuming that the Havnes parameter  $P = ZN/n_e$  is fairly small (“rarefied” particle clouds). This allows us to neglect changes in the rf plasma composition due to the presence of charged microparticles. For our experimental conditions, this approach is well justified: The initial value of the parameter is  $P_0 \sim 0.1$ . The subsequent decrease of the charge leads to a reduction of  $P$  down to  $\sim 10^{-3}$ . Therefore, the plasma diffusion in the cloud is ambipolar until the plasma

density falls off 3 orders of magnitude from its initial value. Further diffusion of ions will be stopped by the electric field created due to the (comparatively) motionless charged microparticles, whereas the electron diffusion will go on. Therefore, the cloud quasineutrality at this stage is provided by ions, and the ion-to-electron density ratio  $n_i/n_e \approx P$  grows with time. Equation (6) shows that in this case  $Z$  should decrease gradually and tend asymptotically to zero [15]. However, we do not observe this in the experiment. The reason is the presence of the excitation electric field,  $E_{\text{FG}} \sim 10$  V/cm (vacuum value). This field is much stronger than the field that might be created by the charged particles, which can be estimated as  $\leq 2\pi e Z_{\text{rest}} N \Delta \sim 0.5-1$  V/cm ( $\Delta \sim 3-5$  mm is the thickness of the particle layer). At the initial stage of the plasma decay, the excitation field is significantly diminished in the cloud due to the plasma screening ( $\lambda_{i0} \sim 10-30$   $\mu\text{m}$  is much smaller than  $\Delta$ ) and hence does not affect the plasma diffusion. As the plasma density decreases by a factor of  $\sim 10^3$  from its initial value,  $\lambda_i$  becomes comparable with  $\Delta$  and the charged particles cannot retain the ions in the cloud any longer: Ions drift towards the electrode following the excitation field, leaving the microparticles with the rest charge.

This work was supported by DLR under Grant No. 50WM9852. The authors acknowledge the excellent support from the PKE team (quoted in [11]).

- 
- [1] H. Thomas *et al.*, Phys. Rev. Lett. **73**, 652 (1994).
  - [2] J. H. Chu and Lin I, Phys. Rev. Lett. **72**, 4009 (1994).
  - [3] Y. Hayashi and K. Tachibana, Jpn. J. Appl. Phys. **33**, L804 (1994).
  - [4] H. M. Thomas and G. Morfill, Nature (London) **379**, 806 (1996).
  - [5] G. E. Morfill *et al.*, Phys. Plasmas **6**, 1769 (1999).
  - [6] G. E. Morfill *et al.*, Phys. Rev. Lett. **83**, 1598 (1999).
  - [7] M. Zuzic *et al.*, Phys. Rev. Lett. **85**, 4064 (2000).
  - [8] P. K. Shukla and A. A. Mamun, *Introduction to Dusty Plasma Physics* (Institute of Physics, Bristol, 2002).
  - [9] A. Piel and A. Melzer, Plasma Phys. Controlled Fusion **44**, R1 (2002).
  - [10] A. P. Nefedov *et al.*, Phys. Rev. Lett. (to be published).
  - [11] PKE team, <http://www.mpe.mpg.de/pke/hardware.html>.
  - [12] S. Khrapak *et al.*, Phys. Plasmas **10**, 1 (2003).
  - [13] B. M. Annaratone *et al.*, Phys. Rev. E **66**, 056411 (2002).
  - [14] F. Melandsø *et al.*, J. Vac. Sci. Technol. A **14**, 619 (1996).
  - [15] O. Havnes, T. Aanesen, and F. Melandsø, J. Geophys. Res. **95**, 6581 (1990).
  - [16] J. P. Boeuf and L. C. Pitchford, Phys. Rev. E **51**, 1376 (1995).
  - [17] V. N. Tsytovich, Phys. Usp. **40**, 53 (1997).
  - [18] Yu. P. Raizer, *Gas Discharge Physics* (Springer, Berlin, 1991).
  - [19] F. Melandsø, T. Aslaksen, and O. Havnes, Planet. Space Sci. **41**, 321 (1993).